

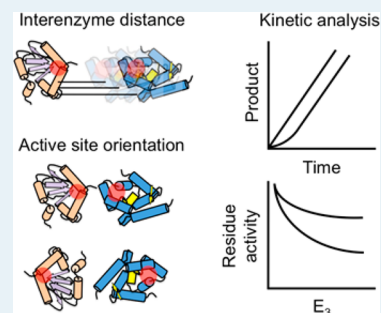
Design and Analysis of Enhanced Catalysis in Scaffolded Multienzyme Cascade Reactions

Jyun-Liang Lin, Leidy Palomec, and Ian Wheeldon*

Department of Chemical and Environmental Engineering, University of California, Riverside, Bourns Hall, 900 University Avenue, Riverside, California 92521, United States

ABSTRACT: New developments in nucleic acid nanotechnology and protein scaffold designs have enabled unparalleled control over the spatial organization of synthetic multienzyme cascade reactions. One of the goals of these new technologies is to create nanostructured enzyme cascade reactions that promote substrate channeling along the cascade and, in doing so, enhance cascade catalysis. The concept of substrate channeling has a long and rich history in biochemistry and has established methods of evaluation and quantification. In this Perspective, we review the most common of these methods and discuss them in the context of engineered multienzyme systems and natural bifunctional enzymes with known mechanisms of substrate channeling. In addition, we use experimental data and the results of simulations of coupled-enzyme reactions to develop a set of preliminary design rules for engineering multienzyme nanostructures. The design rules address the limitations on interenzyme distance and active site orientation in substrate channeling and suggest designs for promoting enhanced catalysis, specifically, that enzyme orientation should minimize interenzyme distance and that at distances greater than 1 nm between active sites, significant channeling occurs only if diffusion of the intermediate is bounded through interactions with the surface or scaffold between active sites. This field is rapidly developing and promises to create many more new and exciting technologies.

KEYWORDS: multienzyme, cascade, enzyme scaffold, substrate channeling, enzyme kinetics, DNA nanostructures, protein engineering



1. INTRODUCTION

The multistep reaction cascades of cellular metabolism are highly coordinated, simultaneously processing a battery of biosynthetic and oxidative pathways to build essential biomolecules and catabolize energy sources. One strategy that has evolved to allow for this to occur within the confined environment of a single cell is substrate channeling along spatially organized multienzyme structures. Substrate channeling is the transfer of a reaction intermediate from the active site of one enzyme to the active site of a downstream enzyme without first diffusing to the bulk solution. This is an important phenomenon that can result in sequestering substrates and intermediates along specific pathways, thus increasing pathway flux and minimizing cross-talk between separate pathways.

Substrate channeling has a long history in biochemistry with many interesting discoveries, and like many fields, it is not without controversy in the analysis of experimental evidence and in the existence of different mechanisms.^{1–3} The past 5 years have seen a re-emergence of this topic, with a focus on engineering nanostructured assemblies for coupled-enzyme reactions and colocalization scaffolds for biosynthetic pathways.^{4–7} At the root of these efforts is the desire to engineer enzyme reaction cascades with enhanced catalysis. Systems are designed to promote substrate channeling and control the local concentration and flux of reaction intermediates and, in doing so, increase reaction rates, prevent undesired side reactions from consuming intermediates, and drive reactions counter to unfavorable thermodynamics in the bulk environment.

Inspired by natural metabolic pathways and bifunctional enzymes, researchers are developing new strategies to create colocalized and spatially organized multienzyme structures (Figure 1). Using protein, nucleic acid, and polymer scaffolds to position enzymes in multienzyme structures, enhancements in overall reaction cascade kinetics have been demonstrated both *in vivo* and *in vitro*. For example, a modular DNA scaffold expressed in *Escherichia coli* has produced a 5-fold increase in *trans*-resveratrol yield from a coupled enzyme reaction;⁸ colocalization of a two-enzyme system using protein and RNA scaffolds has produced up to 50-fold increases in the production of biohydrogen in *E. coli*;^{9,10} a protein scaffold used to assemble a three-enzyme mevalonate pathway resulted in a 77-fold increase in yield;¹¹ and two separate examples of DNA scaffolds used to colocalize a model coupled-enzyme reaction *in vitro* demonstrate a >15-fold increase in the initial pathway reaction rate.^{12,13} The prevailing reasoning used to explain enhancements due to colocalization is that when enzymes are assembled in close proximity, enhancements in catalysis are due to an increased local concentration of reaction intermediates. At low intermediate concentration, the second enzyme of a coupled reaction is pseudo-first-order with respect to the intermediate; thus, increases in local concentrations increase the reaction velocity.¹⁴ An alternative mechanism of yield

Received: October 31, 2013

Revised: December 17, 2013

Published: December 19, 2013

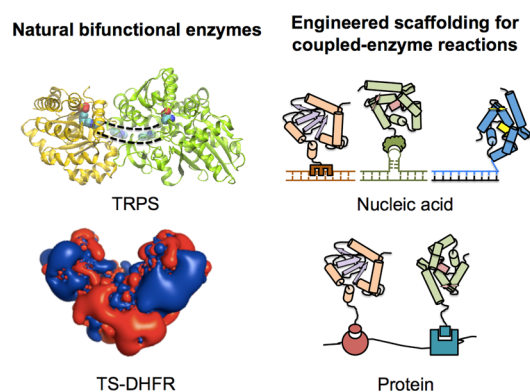


Figure 1. Natural strategies of substrate channeling in bifunctional enzymes and engineering approaches to colocalizing enzymes in a cascade reaction. (top, left) Crystal structure of tryptophan synthase (TRPS) with intramolecular tunnel (dashed lines) that connects the active site of the α -subunit to the active site in the β -subunit.²⁰ (bottom, left) Crystal structure of thymidylate synthase–dihydrofolate reductase (TS-DHFR) bifunctional enzyme. The structure is shown with an overlay of the electrostatic map (negative charge shown in red, positive charge shown in blue). The electrostatic interactions between enzyme and negatively charged cascade intermediate promote diffusion between active sites. Adapted with permission from ref 25. (top, right) Examples of enzymes attached to nucleic acid scaffolds, including, from left to right, a DNA binding protein fused to an enzyme, aptamer attachment, and chemical conjugation of an enzyme to a nucleic acid strand. (bottom, right) Two enzymes attached to a protein scaffold by unique protein binding domains fused to the enzyme termini.

enhancement may be at work in vivo: in pathways with toxic intermediates, it is possible that high local enzyme concentrations ensure that intermediates are largely consumed prior to diffusing from the colocalized pathway, thus conferring a fitness benefit in comparison with microorganisms with freely diffusing pathway enzymes.⁴

These new examples of enhanced catalysis in engineered multienzyme structures are important and encouraging, but many challenges remain in developing generalizable systems for assembling multienzyme pathways or cascades with optimized kinetics. For example, accurate positioning and orientation of enzymes at the nanometer scale remains technically challenging, and the diversity of enzyme structures, from primary amino acid sequence to quaternary structure, can prevent broad application of a single strategy for assembly of arbitrary multienzyme cascades. These and more challenges continue to be defined and are being addressed with new strategies to create spatially organized, multienzyme systems with well-defined nanoscale architectures (reviewed in refs 15 and 16).

In this Perspective, we describe recent advances in engineering spatially organized, multienzyme systems in the context of methods of evaluating changes in coupled-enzyme catalysis and, by extension, cascade reactions. We focus on established methods from the biochemistry community to observe and quantify substrate channeling and coupled-enzyme kinetics, and we apply these methods to newly developed spatially organized, multienzyme systems. As a point of comparison, we discuss selected natural examples of bifunctional enzymes with known mechanisms of substrate channeling. Our discussion focuses on in vitro examples because the complexity of the intracellular environment often prevents detailed kinetic analysis and a full understanding of the system architecture is difficult to obtain. On the basis of

published experimental data and simulations of such systems, we describe a preliminary set of design rules (in terms of spatial organization, active site orientation, and scaffold design) for engineering multienzyme systems with enhanced catalysis.

2. SUBSTRATE CHANNELING IN NATURE

Substrate channeling in natural metabolic pathways is not uncommon. In plant biochemistry, many secondary metabolites, including isoprenoids, alkaloids, and flavonoids, are produced by spatially organized pathways assembled, sometimes transiently, on lipid membranes.¹⁷ These enzyme complexes create multistep reaction cascades with optimized ratios of rates and overall structures that create optimal local conditions to protect cells from toxic intermediates and drive pathway catalysis.¹⁸ Channeling and spatial organization also occur at the protein level. The canonical example is the bifunctional enzyme tryptophan synthase, whose active sites are linked by an intraenzyme molecular tunnel through which the reaction intermediate can pass (Figure 1, top, left). Similar intramolecular channels are also found in carbamoyl-phosphate synthetase and glutamine phosphoribosylpyrophosphate amidotransferase (GPTase).^{19,20} Bifunctional aldolase–dehydrogenase complexes are another example of coupling active sites through intraenzyme tunnels.²¹ In this case, the open-ended barrels of each enzyme are genetically fused, sequestering the toxic aldehyde intermediate from the bulk solution.

One example that has inspired our research group is the bifunctional enzyme thymidylate synthase–dihydrofolate reductase (TS-DHFR). TS methylates the RNA base dUMP to complete the synthesis of the DNA base dTMP. The synthesis requires a methylated tetrahydrofolate cofactor (Figure 2).

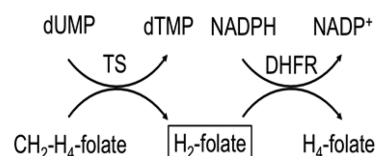


Figure 2. The coupled reaction of TS-DHFR. The dihydrofolate intermediate is boxed for emphasis.

Recycling of the cofactor begins with the reduction of the dihydrofolate product from the TS reaction to tetrahydrofolate at the DHFR active site. The cofactor product of the coupled reaction is subsequently methylated by a third enzyme, serine hydroxymethyltransferase, to complete the cycle. It is in the first step of cofactor recycling that channeling occurs. The TS-DHFR crystal structure of *Leishmania major* reveals a positively charged region on the outer enzyme surface that spans the ~ 4 nm distance between active sites (Figure 1, bottom, left).²² This distance is too far for direct transfer of the intermediate from active site to active site to account for the kinetic behavior of the enzyme, and limited conformational change in protein structure prevents intermediate transfer by a dynamic enzyme–substrate complex mechanism. Brownian dynamic simulations show that the negatively charged dihydrofolate intermediate diffuses between the active sites with high efficiency.²³ Under simulated physiological conditions, the electrostatic interactions between intermediate and enzyme create a zone of bounded diffusion, resulting in $>50\%$ channeling, increasing to $>90\%$ under reduced ionic strength. These simulations are supported by transient and steady-state kinetics that provide evidence of fast intermediate transfer between active sites.²⁴ A recent work

investigating the TS-DHFR bifunctional enzyme from different species reveals that this mechanism of substrate channeling is common among different parasitic protozoa.²⁵

The TS-DHFR example is an important one for engineering of new spatially organized pathways. Structural and kinetic data come together to create a compelling picture of the extent and mechanism of channeling. Because substrate channeling occurs via a bounded diffusion mechanism, channeling is dependent on the chemical and physical environment, and careful analysis was required to clearly identify a mechanism of substrate channeling and the kinetic enhancements due to that mechanism.

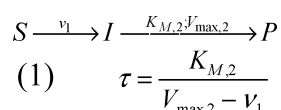
3. KINETIC ANALYSIS OF SUBSTRATE CHANNELING

There have been substantial efforts made to understand the kinetics of coupled enzyme reactions, both with and without the potential occurrence of substrate channeling.^{26–28} Analysis of channeling often focuses on one or more of the following: (1) transient time of the overall reaction, (2) pathway resistance to a competing side reactions, and (3) enhancement in the initial pathway reaction rate. Isotope dilution/enrichment studies and pre-steady-state kinetic analysis can also be used to evaluate possible channeling but can be technically challenging and may not be applicable to all coupled-enzyme systems. Here, we discuss the more common methods of evaluating coupled-enzyme reactions in the context of bifunctional enzymes and engineered multienzyme systems. We direct readers to a comprehensive review on substrate channeling for a full discussion of all evaluation methods.²⁹

3.1. Transient Time of a Coupled-Enzyme Reaction.

Transient time, τ , is the time required to reach steady-state flux of an intermediate in a coupled reaction and is an observable lag phase prior to reaching steady state velocity in a coupled reaction. If we consider the simple reaction of substrate, S , to product, P , via intermediate, I , (Scheme 1) when Michaelis–

Scheme 1



Menten kinetics apply, τ is dependent on the maximum velocity and the Michaelis constant of the second reaction ($V_{max,2}$ and $K_{m,2}$, respectively) and the reaction velocity of the first reaction (v_1) in the relationship shown in Scheme 1.^{14,29}

The transient time, τ , is of interest because it is readily observable in time course kinetic assays, and decreases in τ can be an indication of increased substrate channeling. To this end, eq 1 has been extended to include a condition of channeling,

$$\tau = \frac{K_{M,2}(1 - p_c p_r)}{V_{max,2}} \quad (2)$$

This equation was developed with the condition that a relatively small concentration of the intermediate escapes to the bulk in comparing with the value of $K_{m,2}$.¹⁴ The channeling probability, p_c , is the probability that the intermediate is transferred from active site to active site without first escaping to the bulk. The reaction probability, p_r , is the probability that a reaction occurs once a substrate–enzyme complex is formed at the second active site prior to dissociation of the complex. Figure 3 shows the graphical calculation of τ from a time course

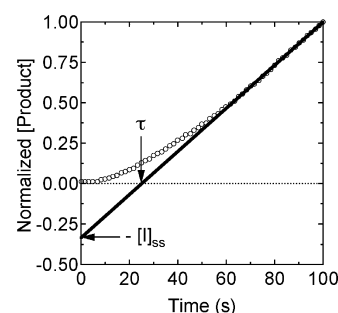


Figure 3. Graphical calculation of the transient time, τ , in a coupled-enzyme reaction. A linear fit to the product concentration as a function of time at steady state crosses the x -axis at τ . The y -intercept is equal to the negative of the steady state concentration of the cascade reaction intermediate, $[I]_{ss}$.

of a coupled reaction. A linear fit to the data crosses the x -axis at τ , and by eq 1, the concentration of the intermediate at steady state is the negative of the y -intercept.

Analysis of the TS-DHFR reaction cascade shows a decrease in τ from 22 s with monofunction DHFR and TS to a τ approaching 0 for the bifunctional enzyme under the same experimental conditions (Figure 4).³⁰ By eq 2, a decrease in τ is indicative of an increase in the extent of substrate channeling in the bifunctional enzyme in comparison with the freely diffusing enzyme pair.

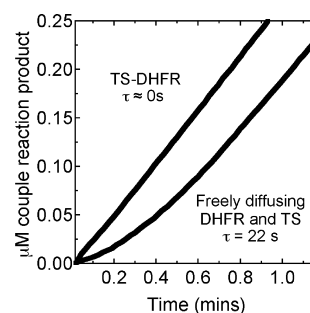


Figure 4. Experimental data of the TS-DHFR bifunctional enzyme and freely diffusing DHFR and TS. Adapted with permission from ref 30. A clear decrease in the transient time can be observed in the bifunctional enzyme in comparison with the freely diffusing enzyme pair.

Changes in τ have also been experimentally observed in an engineered system in which glucose oxidase (GOx) and horseradish peroxidase (HRP) were colocalized on a hexagonal DNA scaffold.¹² This model enzyme pair has been used in a number of DNA scaffold technologies that control colocalization of the coupled reaction. Both GOx and HRP are robust, maintain high activity when modified with chemical cross-linking agents, and make for an excellent model cascade for developing new scaffolds and for exploring the effects of spatial organization and scaffold design on the kinetics of coupled-enzyme reactions (Figure 5). GOx converts glucose and oxygen to gluconolactone and hydrogen peroxide. Hydrogen peroxide is the intermediate of the coupled reaction and is oxidized by HRP with the concomitant reduction of an electron acceptor (in this case, the colorimetric substrate ABTS). A change in the design of the hexagonal DNA scaffold decreases τ from 65 to 45 s. When GOx and HRP are colocalized on the surface of ~ 10 nm diameter micelles, τ is reduced from ~ 25 to < 1 s, indicating a substantial increase in peroxide intermediate directly

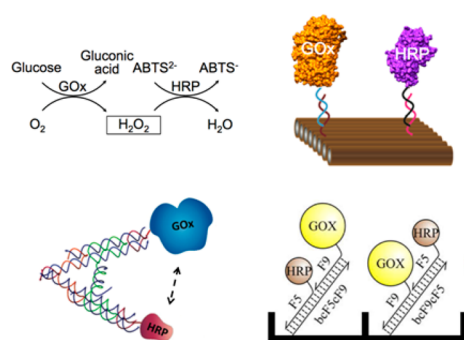


Figure 5. Coupled reaction of glucose oxidase and horseradish peroxidase and examples of DNA scaffolding of the GOx–HRP model cascade. (top, left) Reaction scheme of the coupled GOx–HRP reaction. This model cascade is commonly used to explore new scaffold designs for spatially organized multienzyme structures. (top, right) A cartoon representation of the controlled assembly of GOx and HRP on a DNA origami tile.¹³ (bottom, left) An active DNA scaffold that, with the addition of a DNA “fuel” strand, assembles and disassembles the GOx–HRP cascade. Adapted with permission from reference 39. (bottom, right) Immobilization of the GOx–HRP with DNA strands for the controlled assembly of the GOx–HRP cascade. Adapted with permission from reference 38.

accessing the downstream enzyme prior to diffusing to the bulk.³¹

Given well-defined kinetic parameters, for both freely diffusing enzymes and modified enzymes assembled into spatially organized structures, τ -analysis can be a powerful method of evaluating substrate channeling and enhancements in the kinetics of coupled reactions. Equation 2, as well as similar derivations of kinetic expressions of substrate channelings,^{28,32} can be used to quantify channeling and changes in channeling in a given system.

3.2. Competition for Pathway Intermediates from a Competing Reaction. A relatively straightforward and robust method of evaluating coupled-enzyme reactions is challenging the cascade with a parasitic side reaction whose substrate is the intermediate of interest. The observation of any product from the competing reaction indicates the presence of intermediate in the bulk solution and, therefore, less than perfect channeling in the coupled-enzyme system. The effect of the competing reaction can also be observed in τ . Reaction with the competing enzyme decreases the bulk concentration of intermediate and, consequently, the time required to reach steady state concentrations. These evaluations of channeling (i.e., decreased τ and side product formation) do not require a detailed knowledge of kinetic parameters; however, given such data and an extension of eq 2 to include the third, competing enzyme can be used to quantify the extent of channeling.¹⁴

Challenge from a competing reaction can also affect the overall pathway activity and yield. Figure 6 shows the residual activity of a coupled-enzyme reaction when genetically fused into a single bifunctional enzyme in comparison with a freely diffusing enzyme pair.³³ In this experiment, mitochondrial malate dehydrogenase (mMD) and citrate synthase (CS), a coupled reaction from the Krebs cycle that converts malate to citrate via an oxaloacetate intermediate, are fused N- to C-terminus with a three-amino-acid linker. A model of the mMD–CS fusion protein derived from crystal structures of each individual enzyme shows that an electrostatic patch bridges the protein surface from the mMD active site to the CS active site, a distance of ~ 6 nm. With a high concentration of

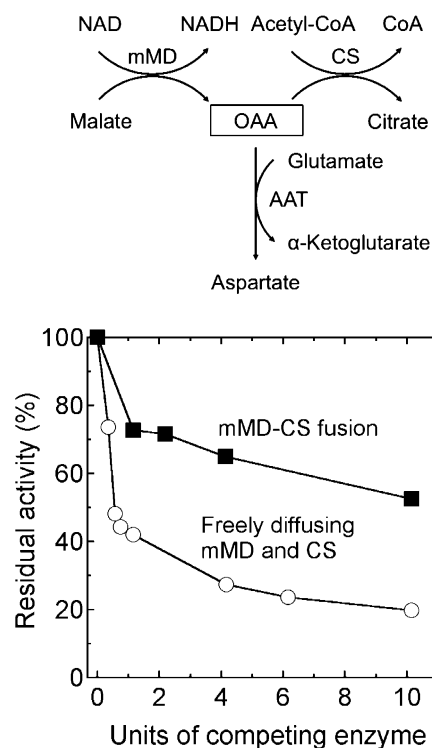


Figure 6. Residual activity of the coupled-enzyme reaction of malate dehydrogenase and citrate synthase in the presence of a freely diffusing enzyme that competes for the coupled reaction intermediate. (top) The coupled reaction of mMD and CS with a competing reaction from aspartate transaminase (AAT). (bottom) A fusion between mMD and CS maintains nearly 60% of maximum activity in the presence of 10 units of competing enzyme, whereas the freely diffusing enzyme pair is reduced to $\sim 20\%$ activity. Adapted with permission from ref 33.

aspartate transaminase (AAT) competing for the oxaloacetate intermediate, the mMD–CS fusion maintains upward of 60% activity. Under the same conditions, freely diffusing enzymes maintain no more than 20% of the maximum activity, indicating that channeling occurs in the enzyme fusion. Combined with Brownian dynamics simulations showing the importance of electrostatics in mMD–CS channeling,^{14,34} the structural data and competition assays present compelling evidence of substrate channeling in the fusion protein.

The presence of a competing reaction can also affect the yield of the desired cascade. For example, an aptamer-based DNA scaffold that assembles GOx and HRP in close proximity protects the peroxide intermediate from a competing reaction with catalase.³⁵ In the presence of catalase, the reaction yield of the assembled GOx–HRP structure is decreased by 20%, and the decrease is upward of 50% under the same conditions with freely diffusing, unassembled GOx and HRP. The resistance of the assembled pathway to the competing reaction is consistent with the concept of channeling by close proximity.

Similarly, the yield of the coupled reaction of bifunctional aldolase–dehydrogenase complexes was used to evaluate substrate channeling. The aldolase cleaves 4-hydroxy-2-oxoacids, producing pyruvate and an aldehyde. The aldehyde intermediate travels through an intramolecular tunnel and is converted to acyl-CoA at the active site of the coupled dehydrogenase. A freely diffusing aldehyde dehydrogenase that converts aldehydes to carboxylates competes for the aldehyde intermediate. The competition assays revealed that upward of 90% of various chain length aldehyde intermediates are

channeled from aldolase to the dehydrogenase.³⁶ This natural bifunctional enzyme is another important example of kinetic and structural data combining to reveal the extent and mechanism of substrate channeling.

3.3. Enhancement in Initial Reaction Rate. The overall reaction rate of a coupled-enzyme reaction is the sum of rates from reaction with intermediates that take a direct route from active site to active site (i.e., intermediates that are channeled) and from intermediates that diffuse to the bulk prior to reaching a downstream active site. At steady state, in the absence of side reactions, and when intermediate decomposition is negligible, this overall rate is not affected by substrate channeling.^{14,28} Similarly, the overall rate of a multienzyme cascade is not affected by substrate channeling and is limited by the maximum rate of the slowest reaction step. The data presented in Figure 4 from the TS–DHFR example demonstrates this point: the slope of the time course data at times $> \tau$ are equal, corresponding to a steady-state rate of $\sim 0.25 \mu\text{M}/\text{min}$.³⁰ Similarly, in analyzing GOx–HRP experimental data, we estimate the rates resulting from two different DNA scaffolds to be equal ($\sim 8 \mu\text{M}/\text{s}$) at times $> \tau$ (46 and 65 s).¹²

The situation is more complex at times $< \tau$ when a coupled-enzyme reaction has yet to reach steady state. At times $< \tau$, the contributions of channeling toward the overall rate can dominate and can result in significant enhancements to the observed overall reaction rate. Modeling and simulation of coupled-enzyme reactions support this idea and demonstrate that the initial enhancement in overall rate can range from $< 1\text{s}$ to tens of minutes, depending on system architecture and reaction volume.³⁷

Enhancements in overall initial rate have also been experimentally observed. For example, a DNA origami tile that colocalizes GOx and HRP at $\sim 10 \text{ nm}$ interenzyme distance results in a > 15 -fold increase in initial pathway reaction rate (Figure 5, top, right).¹³ A 3-fold enhancement in initial rate was demonstrated with the same enzyme pair assembled in close proximity with surface-tethered linear DNA scaffolds (Figure 5, bottom, right).³⁸ Enhancements in overall rate have also been demonstrated with a dynamic scaffold that repeatedly closes (high activity) and opens (low activity) the GOx–HRP reaction cascade (Figure 5, bottom, left).³⁹ Finally, the GOx–HRP coupled reaction shows significant enhancement in overall rate when colocalized inside of a DNA nanotube.⁴⁰

In the emerging field of DNA scaffolds, the predominant model cascade has been GOx–HRP; however, a number of different multienzyme cascades have been assembled using protein scaffolds (Figure 7). For example, three enzymes from the glycolysis pathway (triosephosphate isomerase, aldolase, and fructose 1,6-biphosphatase) were assembled with a dockerin/cohesin-based protein scaffold. The assembled multienzyme cascade produced a > 20 -fold increase in initial rate, in comparison with freely diffusing enzymes.⁴¹ A similar scaffold was used to assemble a cascade of dehydrogenases to oxidize methanol to CO_2 .⁴² Catalytic enhancement of the assembled cascade was observed by a 5-fold increase in the rate of enzyme cofactor production in comparison with an unassembled control. Finally, a trimeric ring-shaped protein made from proliferating cell nuclear antigens (PCNAs) was used as a scaffold to assemble a redox reaction cascade of cytochrome P450 with P450 electron transfer proteins ferredoxin and ferredoxin reductase. The assembled cascade exhibited a 50-fold increase in initial activity over the unassembled control.⁴³ In

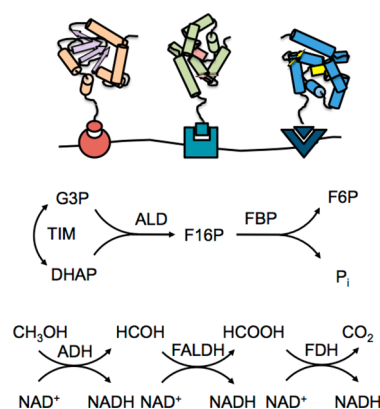


Figure 7. Protein scaffolds and examples of engineered multienzyme cascades. (top) Cartoon representation of a three enzyme cascade assembled by protein–protein interactions on a protein scaffold. (middle) Reaction scheme for the 3-step conversion of glucose-3-phosphate to fructose-6-phosphate. (bottom) Reaction scheme for the 3-step conversion of methanol to carbon dioxide.

each of these protein scaffolding examples, the overall structure of the scaffolded cascade is not well-known. Flexible protein scaffolds allow enzymes to aggregate and form a cluster of enzymes in close proximity. Interenzyme distance and orientation are likely variable, thus preventing clear identification of a mechanism of potential substrate channeling.

4. PRELIMINARY DESIGN RULES FOR ENGINEERING ENHANCED CATALYSIS IN NANOSTRUCTURED MULTIENZYME CASCADES

Newly developed nucleic acid, protein, and polymer scaffolding technologies have enabled the design and engineering of multienzyme cascade reactions with control over the positioning of cascade enzymes and the overall architecture of the multienzyme structure. From the kinetic analysis of these multienzyme structures and of natural bifunctional enzymes that exhibit substrate channeling, we aim to extract a preliminary set of rules for designing new multienzyme cascades. This set of design rules addresses interenzyme distance, active site orientation, and overall architecture of coupled-enzyme structures for promoting substrate channeling. We present these guidelines and design rules as a preliminary set and do not expect them to account for differences in specific reaction mechanisms. We recognize that there remains significant technical challenges to the precise positioning of multiple enzymes at the $< 1\text{--}10 \text{ nm}$ scale and in the control of active site orientation. As such, we expect that as the set of available tools used to create spatially organized multienzyme structures improves, new experiments will reveal refinements to the design rules as well as reveal new guidelines not proposed here.

4.1. Interenzyme Distance. Both experimental observations and molecular simulations of coupled-enzyme reactions show us that the distance between enzymes has a significant effect on the proportion of intermediate that takes a direct path from upstream to downstream active sites. Studies of the TS–DHFR and mMD–CS bifunctional enzymes show that channeling can occur with active site distances of up to 6 nm when aided by electrostatic interactions that promote a diffusional path.^{14,34} In the absence of electrostatic interactions in the intervening space between enzymes, Brownian dynamics simulations of two fixed-position enzymes suggest the

probability that the products of the first reaction channels to the second active site is >90% at 0.5 nm, decreasing to <10% at a distance of 4 nm, given optimal orientations of the active sites.⁴⁴ Many experimental examples that bring enzymes in close proximity (i.e., that are assembled in a structure where upstream and downstream enzymes are essentially in contact) are consistent with these simulation results. For example, when the GOx–HRP cascade is assembled with 10 nm between flexible tethers on a DNA origami tile, a 15-fold increase in the initial rate is observed. The flexibility of the tethers allows for GOx and HRP to come into contact.¹³ Similarly, flexible protein scaffolds allow cascade enzymes to cluster, resulting in enhanced initial rates.^{41–43}

When taken together, the experimental and simulation data describing substrate channeling as a function of the distance between active sites suggests that at fixed distances between active sites greater 1–2 nm, substrate channeling occurs to a significant extent only if diffusion between active sites is promoted by interactions between the cascade intermediate and the surface or scaffold between the enzymes. This distance can be extended with bounded diffusion between active sites, as is demonstrated in the case of the natural bifunctional enzyme TS–DHFR (~4 nm between active sites) and the fusion of mMD and CS (~6 nm between active sites).

4.2. Enzyme Orientation. Intimately coupled to the effects of interenzyme distance on substrate channeling is the orientation of active sites within a cascade. Natural examples of bifunctional enzymes have inherent control over the positioning of active sites, an ability that still remains as a significant technological challenge in engineering multienzyme structures. Recent works have demonstrated the importance of active site orientation in single-enzyme systems immobilized on a surface⁴⁵ and in electron transfer reactions with electrode-immobilized redox enzymes.⁴⁶ Specific to cascade reactions, Brownian dynamics simulations have been used to describe a relationship between the orientations of the active sites and the probability of the downstream reaction.⁴⁴ At a fixed interenzyme distance of 0.5 nm, inward-facing active sites can limit substrate access to the first enzyme in the cascade, thus reducing the overall throughput of the cascade. At 1 nm spacing, direct alignment of the active sites is optimal and leads to the highest probability that the second reaction in the cascade occurs. Experimental descriptions of the effects of the active site and enzyme orientation on cascade reactions has yet to be developed and represents an important area of future research.

4.3. Multi-Enzyme Architectures. Newly developed enzyme colocalization techniques have only just begun to enable the analysis of spatially organized coupled reactions. As such, there is not an extensive data set from which we can distill detailed, generalizable design rules for assembling multienzyme structures with optimized channeling. However, from established τ -analysis and from simulations and modeling of an engineered GOx–HRP system, we can draw two preliminary guidelines. First, eq 1 provides the simple principle that the rate of the downstream enzyme must be greater than the velocity of the first reaction. Under these conditions, the concentration of the intermediate will attain a steady state value. If the production of the intermediate is greater than the maximum value of its consumption (i.e., $V_{\max,2}$), then a steady state will not be reached and, regardless of channeling, the concentration of the bulk intermediate will increase. With respect to the design of multienzyme nanostructures, this suggests that the

ratio of the upstream enzyme to the downstream enzyme within the cascade should be balanced so that $V_{\max,2}$ is greater than the velocity of the upstream enzyme. Second, modeling and simulation work that describes the kinetic enhancements in an experimental systems that couples GOx and HRP in a hexagonal DNA structure shows that the overall structure of the multienzyme systems has a significant effect on system catalysis.³⁷ Such modeling and simulation efforts are important in understanding these systems and help in our understanding of the kinetics of the systems and the relationships between the system architecture and catalysis.

5. CONCLUSIONS

In this Perspective, we aim to connect new progress in engineering nanoscale multienzyme structures to the methods and analysis techniques that the biochemistry community has established over the past 20 or more years to evaluate the kinetics of coupled-enzyme reactions and substrate channeling. Recent progress in the development of DNA nanotechnologies that create programmable, well-defined structures through Watson–Crick base pairing have enabled the creation of multienzyme nanostructures with a high degree of spatial organization. The enzymes of a coupled reaction can be tethered at known distances down to ~10 nm,¹³ organized into aggregate structures with high enzyme density,¹² assembled on the inside of nanoscale DNA tubes,⁴⁰ and dynamically pushed together and pulled apart.³⁹ Engineerable protein scaffolds that can assemble multienzyme structures with high densities of enzymes and with tunable enzyme ratios compliment these new DNA nanotechnology tools.^{42,47}

Detailed analysis of the kinetics of coupled-enzyme reactions assembled with these DNA and protein technologies is important and promises to reveal how far we have come in mimicking natural bifunctional enzymes and metabolic cascades that rely on substrate channeling to drive pathway flux and protect cascade intermediates from reaction in alternate pathways. Transient time (τ) analysis along with detailed knowledge of the enzyme kinetic parameters can be used to quantitatively evaluate the extent of substrate channeling in a given system. Challenge from a competing reaction in the bulk solution that uses cascade intermediates as substrates can also be used to evaluate channeling and the extent of protection that a multienzyme structure provides to its cascade intermediates. Finally, under pre-steady-state conditions, increases in the overall reaction rate can reveal enhanced catalysis and possibly substrate channeling.

A second goal of this Perspective is to develop a preliminary set of design rules or guidelines for promoting substrate channeling in engineered multienzyme systems. To do so, we evaluate published data on natural bifunctional enzyme systems with strong experimental and modeling evidence supporting the existence of substrate channeling as well as data from new engineered multienzyme systems that demonstrate enhanced catalysis. The preliminary design rules are (1) in the absence of bounded diffusion, interenzyme distances in which substrate channeling can occur to a significant extent is limited to approximately 1 nm; (2) significant substrate channeling can be achieved at interenzyme distances of 5–6 nm if diffusion between active sites is promoted through interactions between the surface between the active sites and the cascade intermediate; (3) at close proximity, active site orientation can block substrate access to the coupled reaction; (4) when substrates can access active sites from the bulk solution, active

site orientation should minimize interenzyme distance; and (5) to achieve a steady state concentration of cascade intermediate, the ratio of enzymes should be balanced so that the velocity of the first reaction is less than the maximum velocity of the second reaction. These general design rules are preliminary, and we expect that as the capabilities of the engineering tools for multienzyme nanostructures improve, these guidelines will be refined and new rules will be discovered.

This set of guidelines and the data sets from which they were drawn also highlight the technological challenges that remain in engineering generalizable tools for the assembly of multienzyme nanostructures with optimized catalysis. New protein and biomolecular engineering tools are needed to create multienzyme systems with precise interenzyme distances in the <1–10 nm range. Similar tools are needed to accurately control the orientations of enzyme active sites. Importantly, many more examples of nanostructured coupled-enzyme reactions are needed so that we can evaluate the effects of new multienzyme architectures as well as the behavior of different enzyme reaction mechanisms in such systems.

Engineering new multienzyme nanostructures with optimized kinetics is a complex and multidisciplinary problem that includes aspects of biophysics and biochemistry, as well as protein, biomolecular, and nanoscale engineering. Recent progress in technology development is encouraging and promises to produce many more interesting discoveries.

AUTHOR INFORMATION

Corresponding Author

*E-mail: iwheeldon@enr.ucr.edu.

Notes

The authors declare no competing financial interest.

ACKNOWLEDGMENTS

This work was supported by the Air Force Office of Scientific Research Young Investigator Program (FA9550-13-1-0184) and the Bourns College of Engineering at the University of California, Riverside.

REFERENCES

- (1) Wu, X. M.; Gutfreund, H.; Lakatos, S.; Chock, P. B. *Proc. Natl. Acad. Sci. U.S.A.* **1991**, *88*, 497–501.
- (2) Chock, P. B.; Gutfreund, H. *Proc. Natl. Acad. Sci. U.S.A.* **1988**, *85*, 8870–8874.
- (3) Srivastava, D. K.; Bernhard, S. A. *Science* **1986**, *234*, 1081–1086.
- (4) Lee, H.; DeLoache, W. C.; Dueber, J. E. *Metab. Eng.* **2012**, *14*, 242–251.
- (5) Zhang, Y. H. *Biotechnol. Adv.* **2011**, *29*, 715–725.
- (6) Conrado, R. J.; Varner, J. D.; DeLisa, M. P. *Curr. Opin. Biotechnol.* **2008**, *19*, 492–499.
- (7) Chen, A. H.; Silver, P. A. *Trends Cell Biol.* **2012**, *22*, 662–670.
- (8) Conrado, R. J.; Wu, G. C.; Boock, J. T.; Xu, H.; Chen, S. Y.; Lebar, T.; Turnsek, J.; Tomsic, N.; Avbelj, M.; Gaber, R.; Koprivnjak, T.; Mori, J.; Glavnik, V.; Vovk, I.; Bencina, M.; Hodnik, V.; Anderluh, G.; Dueber, J. E.; Jerala, R.; Delisa, M. P. *Nucleic Acids Res.* **2011**, *40*, 1879–1889.
- (9) Agapakis, C. M.; Ducat, D. C.; Boyle, P. M.; Wintermute, E. H.; Way, J. C.; Silver, P. A. *J. Biol. Eng.* **2010**, *4*, 3.
- (10) Delebecque, C. J.; Lindner, A. B.; Silver, P. A.; Aldaye, F. A. *Science* **2011**, *333*, 470–474.
- (11) Dueber, J. E.; Wu, G. C.; Malmirchegini, G. R.; Moon, T. S.; Petzold, C. J.; Ullal, A. V.; Prather, K. L. J.; Keasling, J. D. *Nat. Biotechnol.* **2009**, *27*, 753–759.
- (12) Wilner, O. I.; Weizmann, Y.; Gill, R.; Lioubashevski, O.; Freeman, R.; Willner, I. *Nat. Nanotechnol.* **2009**, *4*, 249–254.
- (13) Fu, J. L.; Liu, M. H.; Liu, Y.; Woodbury, N. W.; Yan, H. *J. Am. Chem. Soc.* **2012**, *134*, 5516–5519.
- (14) Elcock, A. H.; Huber, G. A.; McCammon, J. A. *Biochemistry* **1997**, *36*, 16049–16058.
- (15) Fu, J.; Liu, M.; Liu, Y.; Yan, H. *Acc. Chem. Res.* **2012**, *45*, 1215–1226.
- (16) Schoffelen, S.; van Hest, J. C. M. *Soft Matter* **2012**, *8*, 1736–1746.
- (17) Sweetlove, L. J.; Fernie, A. R. *Annu. Rev. Plant Biol.* **2013**, *64*, 723–746.
- (18) Jorgensen, K.; Rasmussen, A. V.; Morant, M.; Nielsen, A. H.; Bjarnholt, N.; Zagrobelny, M.; Bak, S.; Moller, B. L. *Curr. Opin. Plant Biol.* **2005**, *8*, 280–291.
- (19) Huang, X. Y.; Holden, H. M.; Raushel, F. M. *Annu. Rev. Biochem.* **2001**, *70*, 149–180.
- (20) Miles, E. W.; Rhee, S.; Davies, D. R. *J. Biol. Chem.* **1999**, *274*, 12193–12196.
- (21) Carere, J.; McKenna, S. E.; Kimber, M. S.; Seah, S. Y. K. *Biochemistry* **2013**, *52*, 3502–3511.
- (22) Knighton, D. R.; Kan, C. C.; Howland, E.; Janson, C. A.; Hostomska, Z.; Welsch, K. M.; Matthews, D. A. *Nat. Struct. Biol.* **1994**, *1*, 186–194.
- (23) Elcock, A. H.; Potter, M. J.; Matthews, D. A.; Knighton, D. R.; McCammon, J. A. *J. Mol. Biol.* **1996**, *262*, 370–374.
- (24) Liang, P. H.; Anderson, K. S. *Biochemistry* **1998**, *37*, 12195–12205.
- (25) Sharma, H.; Landau, M. J.; Vargo, M. A.; Spasov, K. A.; Anderson, K. S. *Biochemistry* **2013**, *52*, 7305–7317.
- (26) Easterby, J. S. *Biochim. Biophys. Acta* **1973**, *293*, 552–558.
- (27) Easterby, J. S. *Biochem. J.* **1981**, *199*, 155–161.
- (28) Ovadi, J.; Tompa, P.; Vertessy, B.; Orosz, F.; Keleti, T.; Welch, G. R. *Biochem. J.* **1989**, *257*, 187–190.
- (29) Spivey, H. O.; Ovadi, J. *Methods* **1999**, *19*, 306–321.
- (30) Trujillo, M.; Donald, R. G. K.; Roos, D. S.; Greene, P. J.; Santi, D. V. *Biochemistry* **1996**, *35*, 6366–6374.
- (31) Jia, F.; Zhang, Y. J.; Narasimhan, B.; Mallapragada, S. K. *Langmuir* **2012**, *28*, 17389–17395.
- (32) Easterby, J. S. *Biochem. J.* **1989**, *264*, 605–607.
- (33) Shatalin, K.; Lebreton, S.; Rault-Leonardon, M.; Velot, C.; Sreere, P. A. *Biochemistry* **1999**, *38*, 881–889.
- (34) Elcock, A. H.; McCammon, J. A. *Biochemistry* **1996**, *35*, 12652–12658.
- (35) Freeman, R.; Sharon, E.; Teller, C.; Willner, I. *Chemistry* **2010**, *16*, 3690–3698.
- (36) Carere, J.; Baker, P.; Seah, S. Y. K. *Biochemistry* **2011**, *50*, 8407–8416.
- (37) Idan, O.; Hess, H. *ACS Nano* **2013**, *7*, 8658–8665.
- (38) Muller, J.; Niemeyer, C. M. *Biochem. Biophys. Res. Commun.* **2008**, *377*, 62–67.
- (39) Xin, L.; Zhou, C.; Yang, Z.; Liu, D. *Small* **2013**, *9*, 3088–3091.
- (40) Fu, Y. M.; Zeng, D. D.; Chao, J.; Jin, Y. Q.; Zhang, Z.; Liu, H. J.; Li, D.; Ma, H. W.; Huang, Q.; Gothelf, K. V.; Fan, C. H. *J. Am. Chem. Soc.* **2013**, *135*, 696–702.
- (41) You, C.; Myung, S.; Zhang, Y. H. P. *Angew. Chem., Int. Ed.* **2012**, *51*, 8787–8790.
- (42) Liu, F.; Banta, S.; Chen, W. *Chem. Commun.* **2013**, *49*, 3766–3768.
- (43) Hirakawa, H.; Nagamune, T. *ChemBioChem* **2010**, *11*, 1517–1520.
- (44) Bauler, P.; Huber, G.; Leyh, T.; McCammon, J. A. *J. Phys. Chem. Lett.* **2010**, *1*, 1332–1335.
- (45) Liu, Y. W.; Ogorzalek, T. L.; Yang, P.; Schroeder, M. M.; Marsh, E. N. G.; Chen, Z. *J. Am. Chem. Soc.* **2013**, *135*, 12660–12669.
- (46) Xu, S.; Minter, S. D. *ACS Catal.* **2013**, *3*, 1756–1763.
- (47) You, C.; Zhang, Y. H. P. *ACS Synth. Biol.* **2013**, *2*, 102–110.